TRAVELING WAVE FRONT AND ITS FAILURE IN A ONE-DIMENSIONAL ARRAY OF CHUA'S CIRCUITS

by

V. Perez-Munuzuri, V. Perez-Villar, and L. O. Chua

Memorandum No. UCB/ERL M92/39

22 April 1992

TRAVELING WAVE FRONT AND ITS FAILURE IN A ONE-DIMENSIONAL ARRAY OF CHUA'S CIRCUITS

by

V. Perez-Munuzuri, V. Perez-Villar, and L. O. Chua

Memorandum No. UCB/ERL M92/39

22 April 1992

ELECTRONICS RESEARCH LABORATORY

College of Engineering
University of California, Berkeley
94720

TITLE PAGE

TRAVELING WAVE FRONT AND ITS FAILURE IN A ONE-DIMENSIONAL ARRAY OF CHUA'S CIRCUITS

by

V. Perez-Munuzuri, V. Perez-Villar, and L. O. Chua

Memorandum No. UCB/ERL M92/39

22 April 1992

ELECTRONICS RESEARCH LABORATORY

College of Engineering
University of California, Berkeley
94720

TRAVELING WAVE FRONT AND ITS FAILURE IN A ONE-DIMENSIONAL ARRAY OF CHUA'S CIRCUITS

V. Perez-Munuzuri, V. Perez-Villar

Dept. Fisica de la Materia Condensada
Facultad de Fisicas
15706 University of Santiago de Compostela. Spain.

and L.O. Chua

Dept. of Electrical Engineering and Computer Sciences
University of California, Berkeley, CA 94720. USA.

April 1992

Abstract

Traveling wave fronts are considered for a one-dimensional array of Chua's circuits. This solution is obtained analytically and analyzed for the "primary real bifurcation". For diffusion coefficients less than some non-zero critical value it has been observed numerically that the traveling fronts fail to propagate. This nonlinear phenomena is similar to that observed from pulse propagation in nerves, and in coupled continuously- stirred tank reactors.

1. Introduction

Systems of coupled cells with reactions and mass, energy or electric charge transfer often serve as standard models for investigating the phenomena occurring in the transformation and transport processes in living cells, tissues, neuron networks, physiological systems and ecosystems, as well as in all forms of chemical, biochemical and biological reactors and combustions systems. For example, the coupling between a one- dimensional array of CSTRs (Continuously Stirred Tank Reactors) has been used recently to prove the existence of traveling waves in such a medium[1,2]. In the continuous limit, it is possible to get a reaction- diffusion type model which exhibits all the classical properties of an autowave processes: dispersion relation, curvature and so on[3,4].

In recent years, it has become apparent that continuous models can not account for all propagation phenomena occurring in nature. For example, biological experiments in the nerve propagation of a stimuli shows the stimuli can fail to propagate under some conditions. A situation that cannot occur if the medium is a homogeneous continuum. One of the most well known examples is the multiple sclerosis. In this case, traveling wave propagation fails due to insufficient current to stimulate the excitable nerves. The study of wave propagation in systems of excitable cells is an important aspect of neurophysiology and cardiophysiology, for example[5]. It is often the case that propagation failure leads to failure of these systems, and in the case of the cardiac action potential, this can be fatal.

Recently, a significant increase in the number of publications on this subject has appeared[6-9]. In the field of chemistry, recent experiments of Laplante and co-workers[10,11] have shown that a wave initiated in a one- dimensional array of CSTRs

(16 linearly coupled reactors) fails to propagate if the exchange rate is below some non-zero critical value.

To the best of our knowledge, no large arrays exhibiting this effect has been demonstrated or built. In this paper, we propose a more suitable framework for future experiments on traveling waves than those occurring in chemistry and biology. By coupling several Chua's circuit[12,14] (simulating a reaction- diffusion medium) we have been able, first, to show analytically the existence of traveling wave solutions in this system, and second, to observe numerically the same qualitative results on propagation failure as reported in chemistry and biology. The purpose of this paper is to show that the behavior of our system, as a large array of coupled Chua's circuits, is markedly different from the continuous approximation of classical reaction- diffusion models. Moreover, the internal behavior of each circuit/cell proves to be important in the description of the propagation failure phenomena.

The paper is organized as follows: in section II we discuss the circuit model that we will use in the array. Section III provides a stability study of the equilibrium solutions for Chua's circuit when it is coupled with its neighbors. Section IV investigates the existence of traveling wave solutions corresponding to two different nonlinear v-i characteristics (symmetrical and non-symmetrical) for Chua's diode[15] in each circuit cell. The last section is devoted to the analysis of propagation wave failure.

2. Model of Chua's Circuit Array

The basic unit (cell) of our one- dimensional array is a Chua's circuit[16], a simple oscillator which exhibits a variety of bifurcation and chaotic phenomena. The circuit contains three linear energy- storage elements (an inductor and two

capacitors), a linear resistor, and a single nonlinear resistor. Every oscillator was coupled with their adjacent neighbors through linear resistors, simulating a diffusion processes. Fig.1a shows the basic cell circuit as well as the coupling with the adjacent cells, via R-Ohm linear resistors.

The nonlinearity of the Chua's diode is given by the three-segment piecewise-linear resistor characteristic shown in Fig.1b. We will consider the non-symmetrical, as well as the symmetrical Chua's diode in our study of traveling wave fronts.

The circuit dynamics can be described by a third- order autonomous nonlinear differential equation. We have to add a fourth equation which accounts for the coupling between neighbors. In particular, we will choose the dimensionless form given by (1.1) in Ref. [12], which we rewrite for each circuit cell k as,

$$\begin{aligned} \dot{x}_k &= \alpha\,(y_k - h(x_k)) + D\,[x_{k-1} - 2\,x_k + x_{k+1}] \\ \dot{y}_k &= x_k - y_k + z_k \qquad\qquad (k = 0,1,2,\ldots,\ell) \\ \dot{z}_k &= -\beta\, y_k \end{aligned} \tag{1}$$

where h(x) describes the three- segment piecewise- linear curve of the nonlinear characteristic resistor described by $h(x) = a_0 + a_1\,x + b_1\,|x-x_1| + b_2\,|x-x_2|$ when $a_1 = (m_1+m_2)/2$, $b_1 = (m_0-m_1)/2$, $b_2 = (m_2-m_0)/2$, and $a_0 = (m_0-m_1)\,x_1/2 + b_2\,x_2$ or, upon expansion,

$$\begin{aligned} h(x) &= m_2\,x + (m_0 - m_1) && x \geq x_2 \\ &= m_0\,x && x_1 \leq x \leq x_2 \\ &= m_1\,x - (m_0 - m_1) && x \leq x_1 \end{aligned} \tag{2}$$

We will choose $x_1 = -1$ and $x_2 = (m_0-m_1)/(m_0-m_2)$ so that the classical symmetrical situation[12] ($x_2 = 1$) is recovered when $m_2 = m_1$.

In Eq. (1), D represents the diffusion coefficient of variable x, and is given by $\alpha/(G\ R)$ in its dimensionless form[1], where G is the conductance in Siemens of the linear resistor in the Chua's circuit, and R is the coupling resistance in Ohms. The set of fixed parameters used throughout this paper is the assigned values $\{\alpha,\beta,m_0,m_1,m_2\} = \{9,30,-1/7,2/7,1/7\}$ and G = 0.7.

In addition to (1) we impose zero- flux boundary conditions; namely,

$$\partial x(0,t)/\partial s = 0 \ \textit{and}\ \partial x(\ell,t)/\partial s = 0 \qquad (3)$$

where ℓ describes the array length and s is the direction of the diffusion. This is equivalent to assuming $x(0,t) = x(-1,t)$, and $x(\ell,t) = x(\ell+1,t)$, for all $t \geq 0$, when x(0,t) denotes cell 0 and $x(\ell+1,t)$ denotes cell ℓ of the linear array.

The nonlinear boundary- problem described by equations (1) to (3) will be solved by a 4th-order Runge- Kutta with automatic time step size control. The spatial step size is kept at a constant value equal to one. Note that if we take the limit $\Delta s \rightarrow 0$, we would obtain a continuous model, where the *"diffusion"* term of the first equation in (1) represents, then, the Laplacian of x, $\partial^2 x/\partial s^2$.

3. Linear Stability: Primary Bifurcation Branches

The equilibrium states of Eq. (1) obtained by setting $\dot{x}_k = \dot{y}_k = \dot{z}_k = 0$ are

---

[1]We use the same scaled parameters than in Ref. [17].

summarized as follows,

State	x	y	z
P_+	$(m_1-m_0)/m_2$	0	$(m_0-m_1)/m_2$
P_0	0	0	0
P_-	$(m_0-m_1)/m_1$	0	$(m_1-m_0)/m_1$

Here **x**, **y** and **z** are vectors of dimension $(\ell+1) \times 1$. Each of these three equilibrium states represents a solution to Eq. (1) for all values of the parameters. The study of the behavior of the solutions in the neighborhood of the *"trivial"* equilibrium solutions and the questions of their stability are simpler, and, in particular, for the Chua's circuit have been described extensively[12]. Bifurcation of solution branches from the trivial branch is called *"primary bifurcation"* in the literature of traveling waves[18,19]. Only real bifurcations are of interest for us in this paper.

The stability of the trivial solution is determined by the eigenvalues of the linearized equations (1) corresponding to the boundary conditions (3).

The eigenvalues are given by the characteristic polynomial,

$$\lambda^3 + \lambda^2 (1 - \mu_1) + \lambda (\beta - \alpha - \mu_1) - \beta \mu_1 = 0 \qquad (4)$$

where $\mu_1 = -\alpha\, m - D\, (\pi n/\ell)^2$ $(n = 0,1,2,...)$, $m = \{m_0, m_1, m_2\}$ depending on which trivial solution is being considered. (See Appendix A for more details).

Depending on the values of ℓ and D, two regions are found where either all eigenvalues are real, or there are always two complex conjugate roots for (4). This bifurcation line is shown in Fig.2 for n=1. The upper part of the figure corresponds to a saddle point for P_0 and the lower part to a stable focus. The other two trivial

solutions has always two complex eigenvalues with a negative real part (stable focus) for all values of ℓ and D considered in this paper.

4. Traveling Wave Front

Here we investigate the existence of traveling wave solutions of (1) of the form $u(s,t) = u(\xi) = u(s-vt)$, $u = \{x,y,z\}$, for some constant v. In order to have a wave solution which evolves from one $u(P_-)$ to another state $u(P_+)$ (or the reverse), the middle point $u(P_0)$ must be a point of unstable equilibrium[20-22] (corresponding to those already found at the upper part of Fig.2). The interval (P_-,P_0) plays the role of a threshold: exceeding it leads to a transition from state P_- to state P_+ (or the reverse).

To investigate traveling waves having a stationary profile and a constant velocity v, let us define a reference frame moving with the propagating wave whose relative coordinate is defined to be $\xi = s - v\ t$. Eq. (1), thus, transforms into the following system of ordinary differential equations in ξ,

$$-v\ dx/d\xi = \alpha\ (y - h(x))/\varepsilon + D\ d^2x/d\xi^2 \qquad (5)$$

$$-v\ dy/d\xi = x - y + z \qquad (6)$$

$$-v\ dz/d\xi = -\beta\ y \qquad (7)$$

where the subscript k has been dropped to avoid clutter.

Following Ortoleva and Ross[21], we have assumed that x is a fast variable, of order ε^{-1}, whereas for all other variables the relaxation time is of order unity. This approximation is known to reproduce qualitatively quite well the classical results found on traveling waves on reaction- diffusion problems.

The solution of Eqs. (5) to (7) need to be sought in two regions, labeled *"fast"* and *"slow"*, and then joined appropriately. The *"fast"* region is defined to be that interval in the relative coordinate ξ over which rapid (quasidiscontinuous) changes in x take place; the *"slow"* region involves variations on a much larger scale. Applying singular perturbation theory, the Appendix B gives derivations of the following zeroth- order approximate equations for the *"fast"* and *"slow"* regions,

The *"fast"* region,

$$-v\, dx^*/d\xi = \alpha\, (y^* - h(x^*)) + D\, d^2x^*/d\xi^2 \tag{8}$$

$$y^* = \text{const.} \tag{9}$$

The *"slow"* region,

$$\alpha\, (y - h(x)) = 0 \tag{10}$$

$$dy/d\xi - v\, d^2y/d\xi^2 = dx/d\xi + \beta y/v \tag{11}$$

The asterisk indicates here variables in the *"fast"* regions. Eq. (11) has been obtained by differentiating (6) with respect to ξ and using (7). The solutions of equations (8) and (9) must be matched with those of (10) and (11). According to the zeroth- order singular perturbation theory[21], we can formulate the matching conditions only for the solutions from the *"slow"* region. In the problem of front propagation, two *"slow"* regions are separated by a *"fast"* one at some $\xi = \xi_c \in [0,+\infty)$, which means that from the right and the left sides of the *"fast"* region, the *"slow"* variable, y, must be continuous.

Solving equations (10) and (11) in the slow region and imposing the initial conditions at $\xi \to 0$ and $+\infty$, such that the solution remains bounded, we obtain $y = 0$

for the *"slow"* region, at this level of the perturbation theory. In this case, the matching conditions for $\xi = \xi_c$ (*"fast"* region) implies by continuity that $y^* = 0$.

Now, equations (8) and (9) can be solved as a one- variable problem[20-22]. The velocity of the traveling wave solution, v, is obtained by integrating in x^* from $x^* = x_-$ to $x^* = x_+$. Whence we get an expression for v in the form,

$$v = -\alpha \int_{x_-}^{x_+} (y^* - h(x^*))\, dx^* \Big/ \int_0^{\infty} (dx^*/d\xi)^2\, d\xi \qquad (12)$$

The value of v is chosen so that the solution obtained satisfies:

$$(dx^*/d\xi)_{x^*=x_-} = (dx^*/d\xi)_{x^*=x_+} = 0$$

where, in Eq. (12), it is easy to show that $\int_{x_-}^{x_+} (d^2x^*/d\xi^2)\, dx^* = 0$, by the conditions given above.

In this case, the sign of the velocity (direction of the wave) is defined by the upper integral, I, in Eq. (12). The dominant state is defined to be x_- if $I < 0$ and x_+ if $I > 0$. If the integral is equal to zero, then $v = 0$, and the wave front is stationary.

For the symmetrical Chua's diode, where $m_2 = m_1$ in Eq. (2), and imposing the above matching condition, $y^* = 0$, we obtain the value $v = 0$ for the velocity. Fig.3 shows this solution as a stationary wave front. The value of the diffusion coefficient and the length of the linear array were taken such that we are in the upper part of Fig.2. The other possibility (lower part of Fig.2) gives rise to the unstable solution shown in Fig.4 where both initial conditions at P_+ and P_- "fall"

flow towards P_0 and eventually settles to either P_+ or P_- depending on the initial conditions and the chosen parameters.

The non- symmetrical Chua's diode gives more interesting results. In this case, Eq. (12) dues not have a trivial solution and can be completely solved[2],

$$v = \left\{ \frac{4\,\alpha\,D\,I^2}{\hat{x}^2\,(m_2\,\hat{x}^2 - 2\,I)} \right\}^{1/2} \tag{13}$$

where $\hat{x} = x_- - x_+ = (m_0-m_1)(m_1+m_2)/m_1m_2$. From Eq. (13) the maximum allowable value for m_2 is determined by the inequality $I < m_2\,\hat{x}^2/2$; namely, $m_2 = m_1$.

5. Propagation Failure

Solving numerically the Eq. (1) using the non- symmetrical Chua's diode, it is possible to obtain a traveling wave front. A propagating wave can be initiated by setting the first cell at the equilibrium state P_+, while maintaining the remaining cells at P_-. Fig.5 illustrates the result of this simulation for 50 coupled Chua's circuits and a fixed value of the diffusion coefficient (D = 2.57). Observed that as time increases a wave front propagates towards the equilibrium state $x_+ = 3$ from those cells that originated at $x_- = -1.5$. Three different stages can be identified corresponding to the small, intermediate and final regimes of the propagating front. Boundary effects are, in part, responsible for the initial and final regimes. During the intermediate regime, the velocity is constant. In the central portion, the

---

[2]Eq. (9) was solved for $I > 0$. We obtain the bounded solution $x(\xi)$ when $x = x_-$ as $\xi \to 0$ and $x = x_+$ when $\xi \to +\infty$.

propagation can be considered as identical to that observed from an infinite array of discrete cells.

By changing the value of the diffusion coefficient, the velocity changes as was predicted by Eq. (13), although, in contrast to the predictions of the classical theory, the velocity becomes zero at a critical (non-zero) value of the diffusion coefficient D. Fig.6 shows the actual behavior (points) and the theoretical predictions (dashed line) derived from Eq. (13).

Fig.7 shows this critical behavior for a non-propagating wave front below the critical value of the diffusion. After an initial motion (the first 50 sec.) the wave front fails to propagate through more than 7 circuit cells, but rather remains at this stage indefinitely. Observed the constant difference between the circuit cells that have made the transition to P_+ from those which, if unperturbed, will remain at P_-. We notice that propagation fails as a result of blocking transmission (similar to those already found in nerve propagation), and not as a consequence of decreasing amplitude.

J.P. Keener[6,7] proved that the propagation failure is an inherent property of the discrete systems and can not be observed in a continuous, one- variable, homogeneous reaction- diffusion system. In addition, using bifurcation arguments based on the existence of a limit point of a nonuniform steady state, he shows that v approaches zero as D tends to some critical value D^*. It can be shown that,

$$v = \gamma (D - D^*)^{1/2} \qquad (14)$$

where γ and D^* are determined by fitting the numerical data shown in Fig.6 to Eq. (14). Fig.6 shows this solution (continuous line) for $\gamma = 0.529$ and $D^* = 0.363$.

6. Conclusions

We have shown that when several identical Chua's circuits are coupled resistively in a one- dimensional array, traveling wave fronts arise for certain set of parameters. This wave solution is found to move when the Chua's diode is asymmetric. In the symmetrical case, a stationary wave front appears. Both possibilities are analyzed in the context of the primary real bifurcation which gives the minimum length of our array to support a structure at fixed diffusion, D.

At the lowest approximation of the perturbation theory, we have calculated the dependence of the wave velocity on D. This result agrees only qualitatively with the numerical data. Numerically, it has been found that the velocity decreases with D and becomes zero at a critical (non-zero) value, i.e. the wave front fails to propagate.

These differences in behaviors are due to the choice of different models. The smooth asymptotic decay to zero always results when a continuous (PDE) model is used, while an abrupt transition to zero, at a critical, non-zero, value of the diffusion, can only be found in a discrete model where the internal dynamics of each circuit cell plays an important role.

This discrete version of the array of Chua's circuit is being used to generate and study more complicated dynamical patterns, such as those reported by physicist, chemists and biologist in the classical Belousov- Zhabotinsky reaction. Spatial bifurcations as well as spatio- temporal chaos are interesting subjects for future research.

In this paper, we have presented only numerical results. However, large arrays of Chua's circuits can be built via VLSI technology to prove, at real time, its ability as a simpler and lower cost system or model, which is capable of reproducing almost all reaction- diffusion situations described in the literature.

Acknowledgements: VPM thanks J.M. Cruz for helpful discussions and careful reading of this manuscript.

Appendix A

Assumption 1: Let us suppose that $q_0 = \{x_0,y_0,z_0\}$ is a set of equilibrium solution for the Eq. (1) without diffusion. To study the stability of q_0 we will look for the perturbated solutions δq in the form, $q = \delta q + q_0$, where $q = \{x,y,z\}$. Thus, Eq. (1) can be written as,

$$\begin{pmatrix} \dot{\delta x} \\ \dot{\delta y} \\ \dot{\delta z} \end{pmatrix} = \begin{pmatrix} -\alpha\, m & \alpha & 0 \\ 1 & -1 & 1 \\ 0 & -\beta & 0 \end{pmatrix} \begin{pmatrix} \delta x \\ \delta y \\ \delta z \end{pmatrix} + D\, d^2(\delta x)/ds^2 \qquad (A.1)$$

where $m = \{m_0, m_1, m_2\}$, depending on which trivial solution is being considered.

Assumption 2: The solutions of Eq. (A.1) can be written explicitly as uncoupled functions of time and space,

$$\begin{aligned} \delta x &= \exp(\lambda t)\, C_x + F(s)\, \delta x \\ \delta y &= \exp(\lambda t)\, C_y \\ \delta z &= \exp(\lambda t)\, C_z \end{aligned} \qquad (A.2)$$

where C_x, C_y and C_z are unknown functions of {x,y,z} and F(s) accounts for the space solutions.

Substituting (A.2) into (A.1) we get,

$$d^2F(s)/ds^2 + \Gamma\ F(s) = 0 \qquad (A.3)$$

where $\Gamma \in \mathbb{R}^1$, is a function of {x,y,z} and the rest of the parameters of the system appearing in Eq. (A.1). Γ can be explicitly calculated by solving the differential equation (A.3).

$$F(s) = A \cos(\eta\ s - B) \qquad (A.4)$$

where A and B are arbitrary constants and $\eta = |\Gamma|^{1/2}$.

The zero-flux boundary conditions, Eq. (3), used throughout the paper can be easily translated to Eq. (A.4) in the form $dF(s=0)/ds = dF(s=\ell)/ds = 0$. Thus, in Eq. (A.4) the constant B is $p\pi$ and $\eta = n\pi/\ell$ ($p = n = 0,1,2...$).

Since we are interested in the stability of Eq. (1), the eigenvalues, λ, are easily calculated (substituting (A.4) and (A.2) into (A.1)) by solving the equation

$$\begin{vmatrix} -\alpha\ m - (n\pi/\ell)^2 - \lambda & \alpha & 0 \\ 1 & -1-\lambda & 1 \\ 0 & -\beta & -\lambda \end{vmatrix} = 0 \qquad (A.5)$$

Appendix B

We seek stable, physical (nonnegative, bounded) solutions for Eq. (1). We assume that x is a fast variable, of order ε^{-1}, while y and z are supposed to be slow variables. We introduce times τ_f and τ_s for the fast and slow processes, respectively, such that $\tau_f/\tau_s \equiv \varepsilon \ll 1$. The existence of different time scales suggest that we introduce an appropriate scaling transformation so that Eq. (1) becomes Eqs. (5) to (7). We will look for solutions of these equations in the limit $\varepsilon \rightarrow 0$.

The nonlinear traveling wave profile has two characteristic regions; a *"fast"* region where the rapid changes in x takes place, and a *"slow"* region where the rate of the changes in the variables occur on a much larger scale. Doing so, we decompose the problem in these two regions, and match the corresponding solutions at the boundaries.

1. "Fast" region

In order to select terms of like order within this region we introduce a length scale $\lambda(\varepsilon)$ of the order of a diffusion length attained on the short time scale τ_f,

$$\lambda(\varepsilon) = (D\ \tau_f)^{1/2} = (D\ \tau_s\ \varepsilon)^{1/2} \qquad \text{(B.1)}$$

Hence we introduce the scaled relative coordinate ρ, such $\xi = \varepsilon^{1/2}\ \rho$. So that ρ is of order one throughout the *"fast"* region. The velocity of the discontinuity propagation is of the order of the distance $\lambda(\varepsilon)$ divided by the time τ_f. We introduce the reduced velocity $\omega(\varepsilon)$ as $v(\varepsilon) = \varepsilon^{-1/2}\ \omega(\varepsilon)$, and we assume $\omega(\varepsilon)$ to be finite as $\varepsilon \rightarrow 0$. With these assumptions Eqs. (5) to (7) become,

$$D\, d^2x/d\rho^2 + \omega\, dx/d\rho + \alpha\,(y - h(x)) = 0 \qquad \text{(B.2)}$$

$$\omega\, dy/d\rho + \varepsilon\,(x - y + z) = 0 \qquad \text{(B.3)}$$

$$\omega\, dz/d\rho - \varepsilon\,\beta\, y = 0 \qquad \text{(B.4)}$$

Observed that all the terms in Eq. (B.2) are of the same order. This is not the case in Eqs. (B.2) and (B.3). This observation suggests that we construct expansions in ε of $u = \{x,y,z\}$ and velocity $\omega(\varepsilon)$,

$$u = \sum_{n=0}^{\infty}\left\{\varepsilon^n\, u_n(\rho)\right\} \textit{ and } \omega(\varepsilon) = \sum_{n=0}^{\infty}\left\{\varepsilon^n\, \omega_n(\varepsilon)\right\} \qquad \text{(B.5)}$$

To lowest order in ε we obtain the set of coupled differential equations,

$$D\, d^2x_0/d\rho^2 + \omega_0\, dx_0/d\rho + \alpha\,(y_0 - h(x_0)) = 0 \qquad \text{(B.6)}$$

$$\omega_0\, dy_0/d\rho = 0 \qquad \text{(B.7)}$$

$$\omega_0\, dz_0/d\rho = 0 \qquad \text{(B.8)}$$

where Eqs. (B.7) and (B.8) can be solved at this order of the approximation, $y_0 = z_0 = \text{const}$. The values of the constant variables y_0 and z_0 must be determined by matching conditions between the *"fast"* and the *"slow"* regions. Observed that the motion of the traveling wave is described at the lowest order of the perturbation theory, only, by the fast variable.

II. "Slow" regions

Here we choose a new length scale, $\lambda'(\varepsilon)$, associated with the distance over

which the front propagates on the long time scale τ_s,

$$\lambda'(\varepsilon) = \tau_s \, v(\varepsilon) \simeq \tau_s \, \omega_0 \, \varepsilon^{-1/2} \quad as \quad \varepsilon \rightarrow 0 \tag{B.9}$$

and define the length scale transformation $\xi = \varepsilon^{-1/2} \, \phi$. The velocity of propagation is given by Eq. (B.5) and it has been implicitly used in the derivation of Eq. (B.9). Then, Eq. (5) becomes for the *"slow"* region,

$$\varepsilon^2 \, D \, d^2x_0/d\phi^2 + \varepsilon \, \omega_0 \, dx_0/d\phi + \alpha \, (y_0 - h(x_0)) = 0$$

which, that at the zeroth order becomes,

$$\alpha \, (y_0 - h(x_0)) = 0 \tag{B.10}$$

while Eqs. (6) and (7) remain unchanged,

$$\omega_0 \, dy_0/d\phi + x_0 - y_0 + z_0 = 0 \tag{B.11}$$

$$\omega_0 \, dz_0/d\phi - \beta \, y_0 = 0 \tag{B.12}$$

The group of equations corresponding to the solution in the zeroth order of the singular perturbation theory for the regions *"fast"* and *"slow"*, (B.7) to (B.9) and (B.10) to (B.12) respectively, must be fulfilled by matching conditions between both regions, as described in Section 4.

REFERENCES

[1] M. Dolnik and M. Marek. *"Extincion of oscillations in forced and coupled reaction cells"*. J. Phys. Chem. **92** (1988) 2452-2455.

[2] P. Marmillot, M. Kaufman and J.F. Hervagault. *"Multiple steady states and dissipative structures in a circular and linear array of three cells: Numerical and experimental approaches"*. J. Chem. Phys. **95** (1991) 1206-1214.

[3] J.J. Tyson and J.P. Keener. *"Singular perturbation theory of traveling waves in excitable media (a review)"*. Physica **32D** (1988) 327-361.

[4] V.S. Zykov. *"Simulation of wave processes in excitable media"*. Manchester Univ. Press. (1987).

[5] A.C. Scott. *"The electrophysics of a nerve fiber"*. Rev. Mod. Phys. **47** (1975) 487-533.

[6] J.P. Keener. *"The effects of discrete gap junction coupling on propagation in myocardium"*. J. Theor. Biol. **148** (1991) 49-82.

[7] J.P. Keener. *"Propagation and its failure in coupled systems of discrete excitable cells"*. SIAM J. Appl. Math. **47** (1987) 556-572.

[8] C. Balke et al. *"Effects of cellular uncoupling on conduction in anisotropic canine ventricular myocardium"*. Circ. Res. **63** (1988) 879-892.

[9] W.C. Cole, J.B. Picolne and N. Sperelakis. *"Gap junction uncoupling and discontinuous propagation in the heart"*. Biophy. J. **53** (1988) 809-818.

[10] J.P. Laplante and T. Erneux. *"Propagation failure in CSTRs"*. Physica A. *"Proceedings Cong. Brux. Dec. 91"*. F. Baras and D. Walgraef Eds. (1992).

[11] J.P. Laplante and T. Erneux. *"Propagation failure in arrays of coupled bistable chemical reactors"*. Submitted J. Chem. Phys. (1992).

[12] L.O. Chua, M. Komuro and T. Matsumoto. *"The double scroll family, parts I and II"*. IEEE Trans. Circuits Sys. **CAS-33** (1986) 1073-1118.

[13] J. Cruz and L.O. Chua. *"A CMOS IC nonlinear resistor for Chua's circuit"* Submitted IEEE Trans. Circuits Sys. (1992).

[14] L.O. Chua and G.N. Lin. *"Canonical realization of Chua's circuit family"*. IEEE Trans. Circuits SYST. **CAS-37** (1990) 885-902.

[15] M.P. Kennedy. *"Robust Op amp realization of Chua's circuit"*. To appear at Frequenz. **46**(3-4) (1992).

[16] T. Matsumoto. *"A chaotic attractor from Chua's circuit"*. IEEE Trans. Circuits Syst. **CAS-31** (1984) 1055-1058.

[17] T. Matsumoto, L.O. Chua and M. Komuro. *"The double scroll"*. IEEE Trans. Circuits Syst. **CAS-32** (1985) 797-818.

[18] T.J. Mahar and B.J. Matkowsky. *"A model bichemical reaction exhibiting secondary bifurcation"*. SIAM J. Appl. Math. **32** (1977) 394-404.

[19] M. Kubicek and M. Marek. *"Computational methods in bifurcation theory and dissipative structures"*. Springer-Verlag (1983).

[20] S. Koga and Y. Kuramoto. *"Localized patterns in reaction- diffusion systems"*. Prog. Theor. Phys. **63** (1980) 106-121.

[21] P. Ortoleva and J. Ross. *"Theory of propagation of dicontinuities in kinetic systems with multiple time scales: fronts, front multiplicity, and pulses"*. J. Chem. Phys. **63** (1975) 3398-3408.

[22] P.C. Fife and J.B. McLeod. *"The approach of solutions of nonlinear diffusion equations to travelling front solutions"*. Arch. Rational Mech. Anal. **65** (1977) 333-361.

FIGURE CAPTIONS

Figure 1: (a) Chua's circuit consists of a linear inductor L, a linear resistor of conductance G, two linear capacitors C_1 and C_2, and a nonlinear resistor known as the Chua's diode. Each unit is connected to its neighbors through linear resistors R at node V_1. (b) three-segment piecewise- linear v-i characteristic of Chua's diode. The outer regions have slopes m_1 and m_2, and the inner region has slope m_0.

Figure 2: Real bifurcation for the coupled Chua's circuits. The nature of the equilibrium states corresponding to $\{P_-,P_0,P_+\}$ is identified in each region. The formation of spatial structures can only occur in the upper region.

Figure 3: Stationary wave front for the variable x in the symmetrical case (m_2 = m_1 = 2/7). Its shape does not change with time and its velocity is found to be zero. Length of the array is equal to 80 and the coupling resistance is equal to 5 Ω (D = 2.57).

Figure 4: Unstable traveling wave solution. The parameters chosen in this case are found in the lower part of Fig.2. Both initial conditions P_- and P_+ are distributed uniformly along the array (ℓ = 18). The waveforms tend towards P_0 and after some time is attracted by one of the equilibrium states, in this case P_-. Coupling resistance is equal to R = 0.25 Ω.

Figure 5: Propagating wave front moving from Chua's circuit 1 to 50. This front is defined as the wave of transition from state P_- to P_+. The intermediate regime,

far from the boundaries can be considered to have a constant velocity, v = 0.785 circuits by sec. Coupling resistance is equal to R = 5 Ω (D = 2.57).

Figure 6: Propagation failure in a linear array of coupled Chua's circuit. The stationary wave front velocity is clearly seen to approach zero as the diffusion approaches some critical value D^* = 0.363. The points represent the numerical simulation and the continuous line represents their fitting to a quadratic law proposed by Keener. The dashed line is the approximate solution, Eq. (14), in the zeroth order perturbation theory of the continuous case.

Figure 7: Non-propagating wave front for the same numerical conditions as in Fig.5 except R = 27 Ω (D = 0.48). In the first 50 sec. the wave propagates along the array but it fails upon reaching the circuit number 7, where it remains constant from then on.

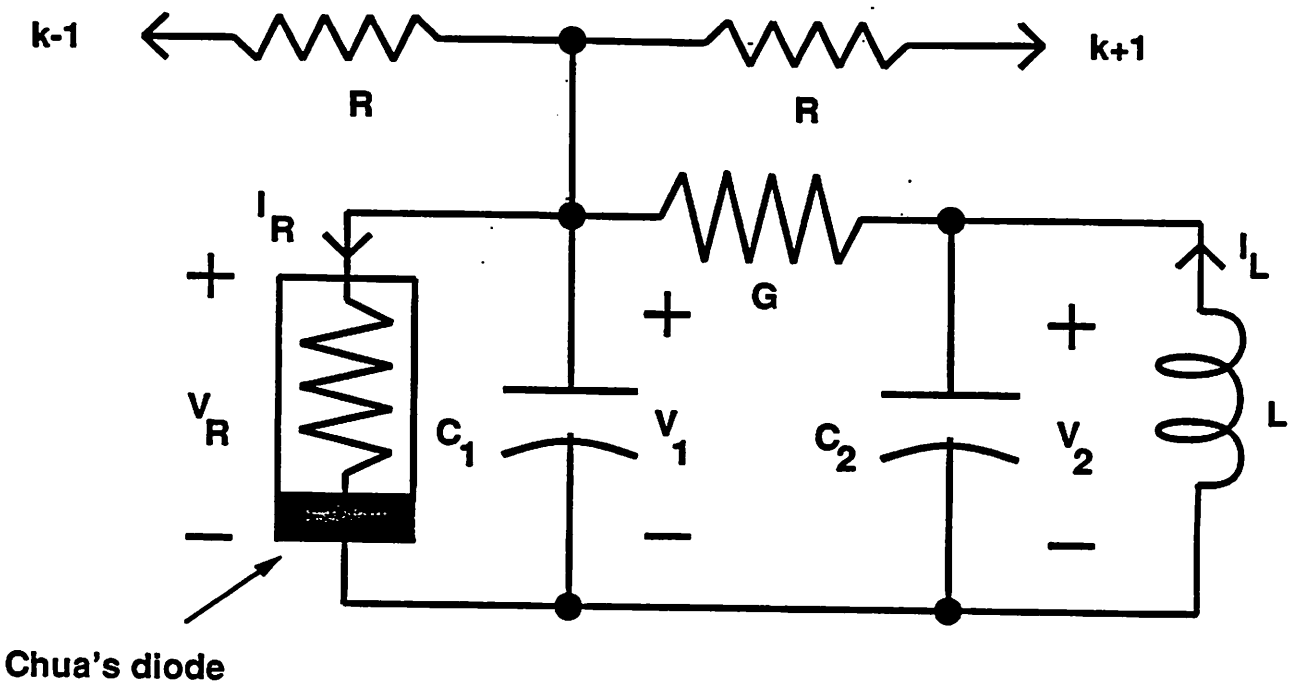

(a)

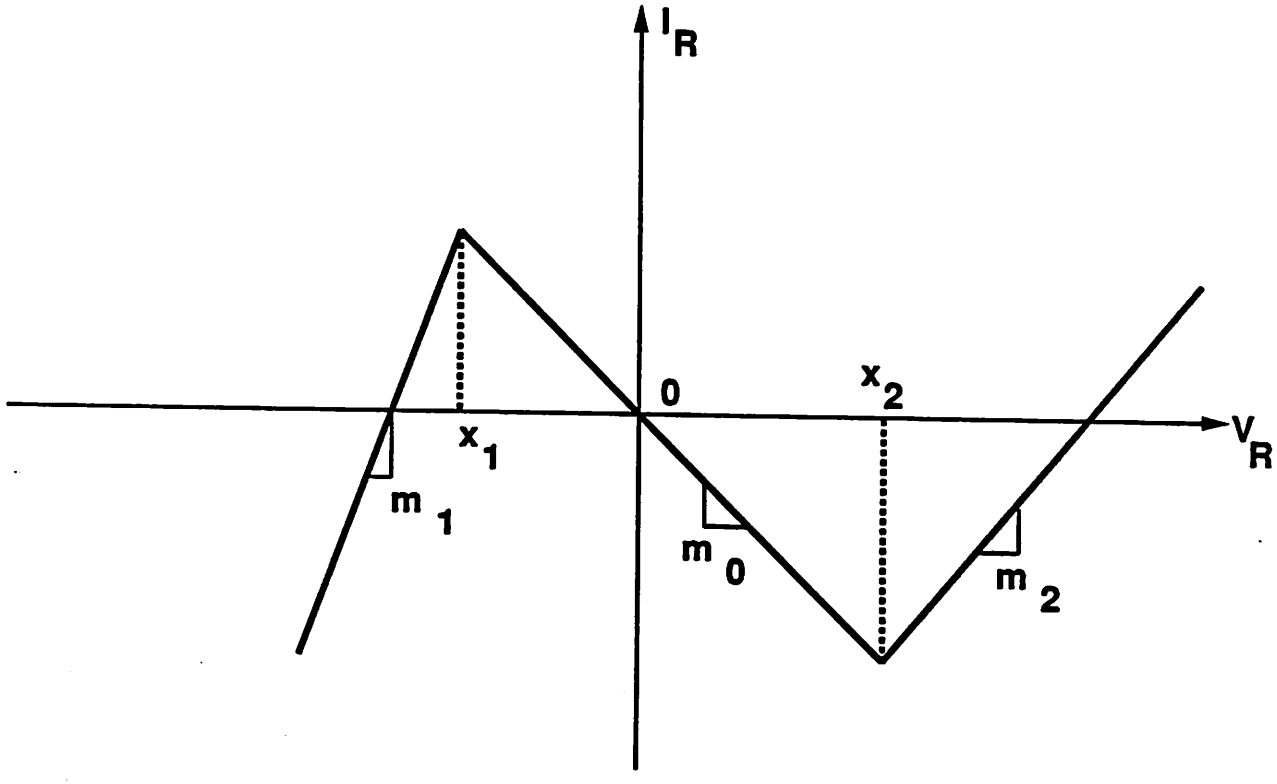

(b)

Figure 1

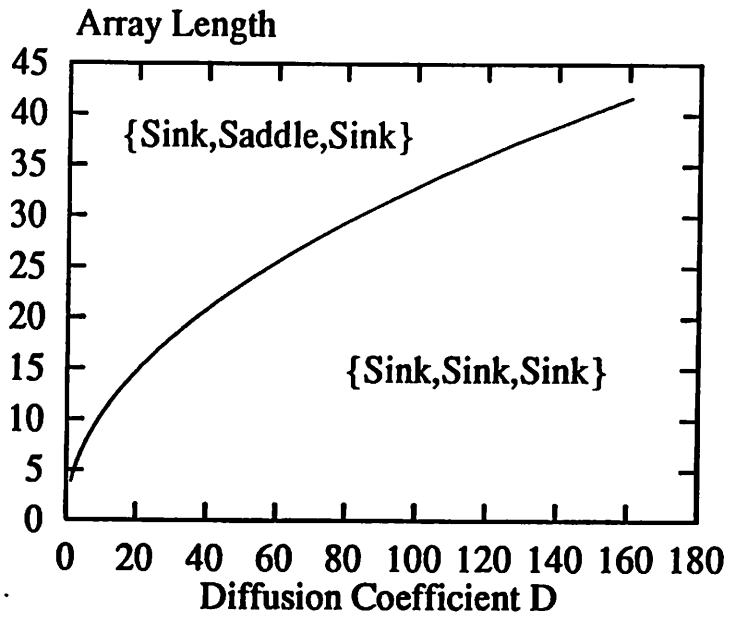
Array Length
45
40
35
30
25
20
15
10
5
0
{Sink,Saddle,Sink}
{Sink,Sink,Sink}
0 20 40 60 80 100 120 140 160 180
Diffusion Coefficient D

Figure 2

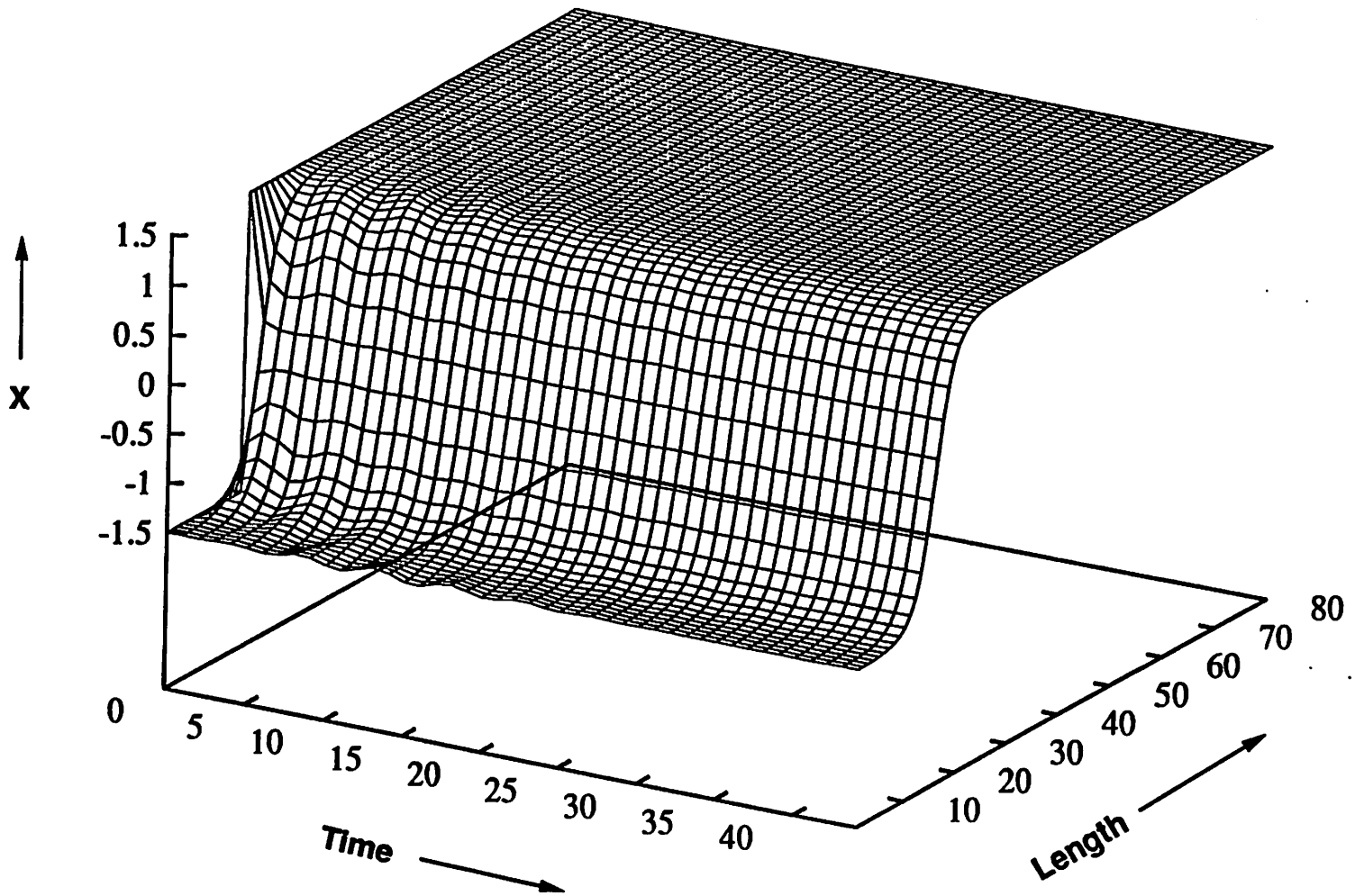
X
1.5
1
0.5
0
-0.5
-1
-1.5
0
5
10
15
20
25
30
35
40
Time
10
20
30
40
50
60
70
80
Length

Figure 3

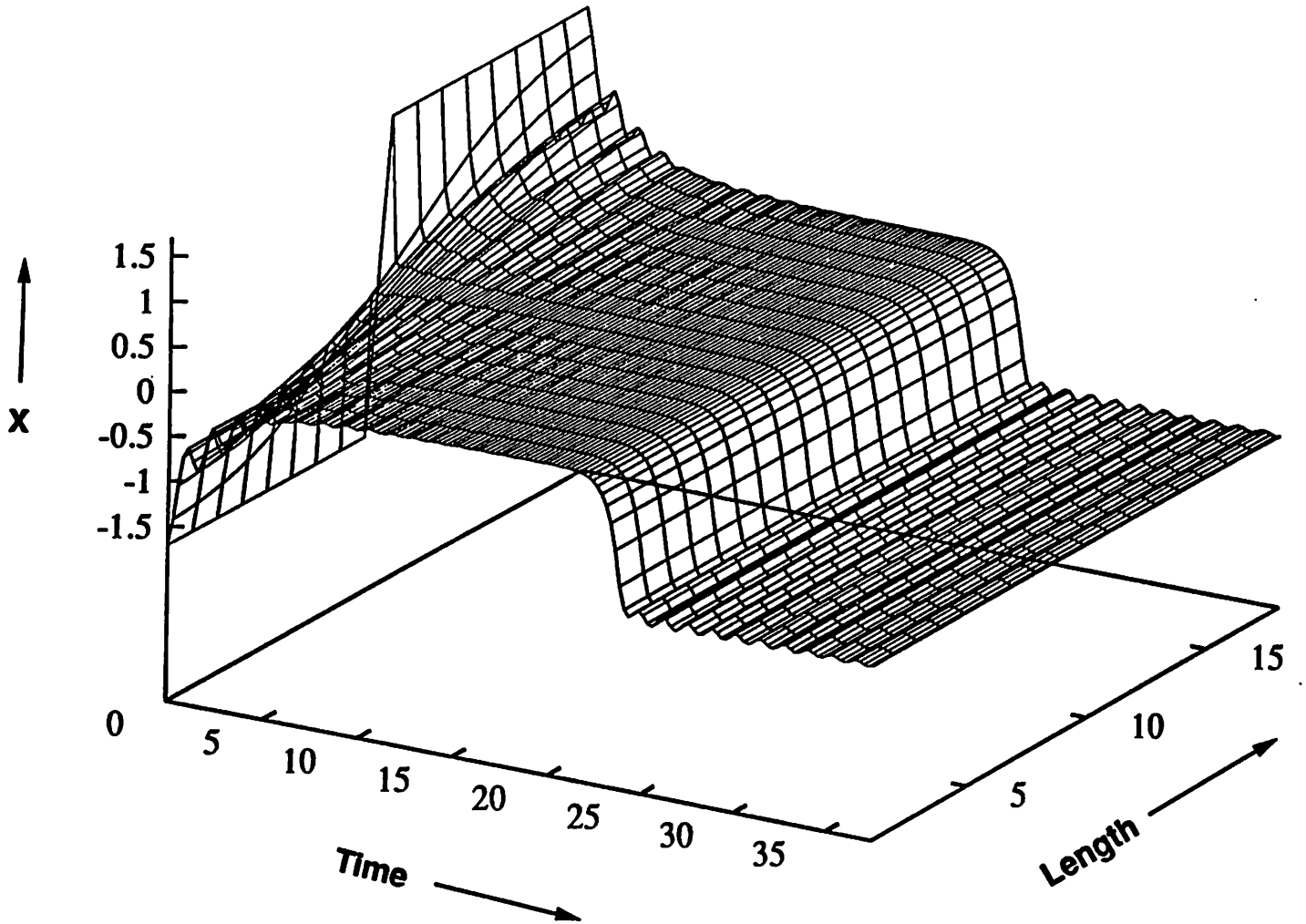

Figure 4

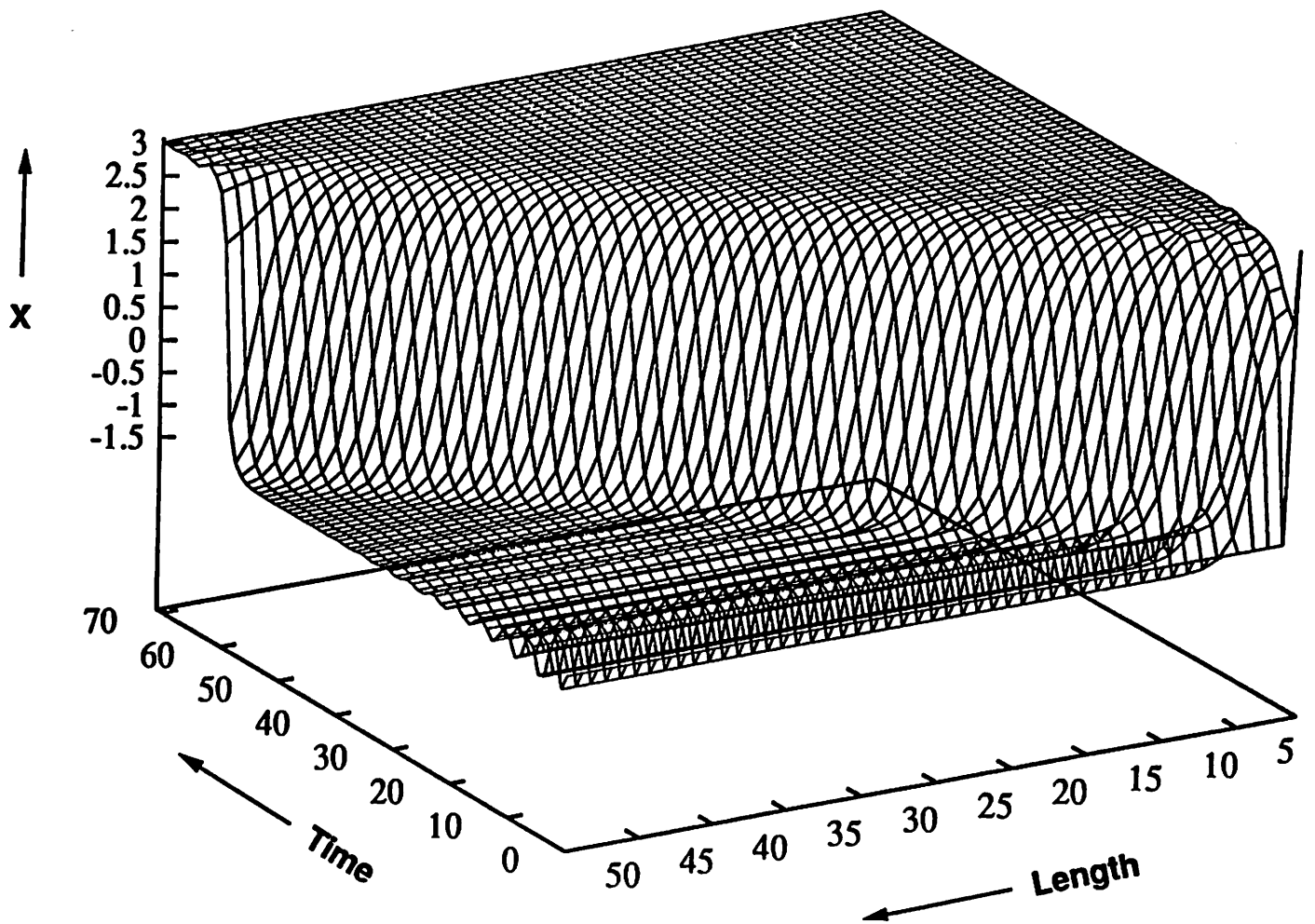
x
3
2.5
2
1.5
1
0.5
0
-0.5
-1
-1.5
70
60
50
40
30
20
10
0
Time
50
45
40
35
30
25
20
15
10
5
Length

Figure 5

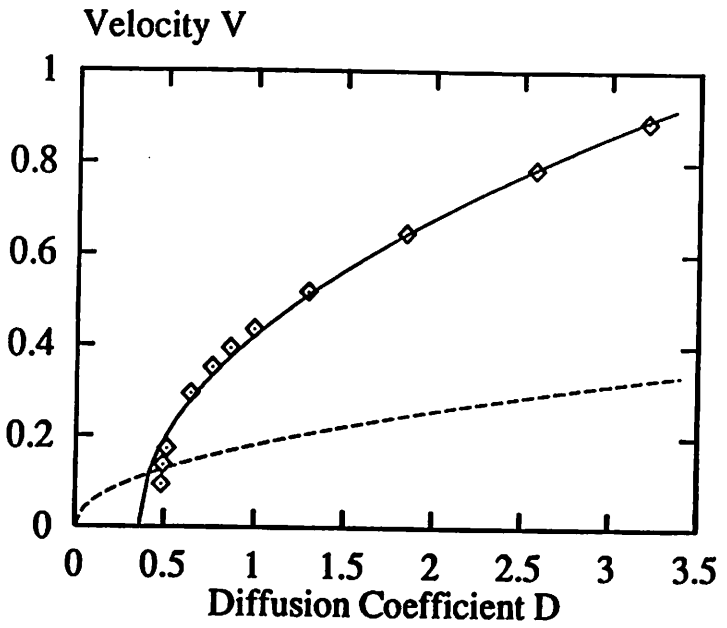
Velocity V
1
0.8
0.6
0.4
0.2
0
0
0.5
1
1.5
2
2.5
3
3.5
Diffusion Coefficient D

Figure 6

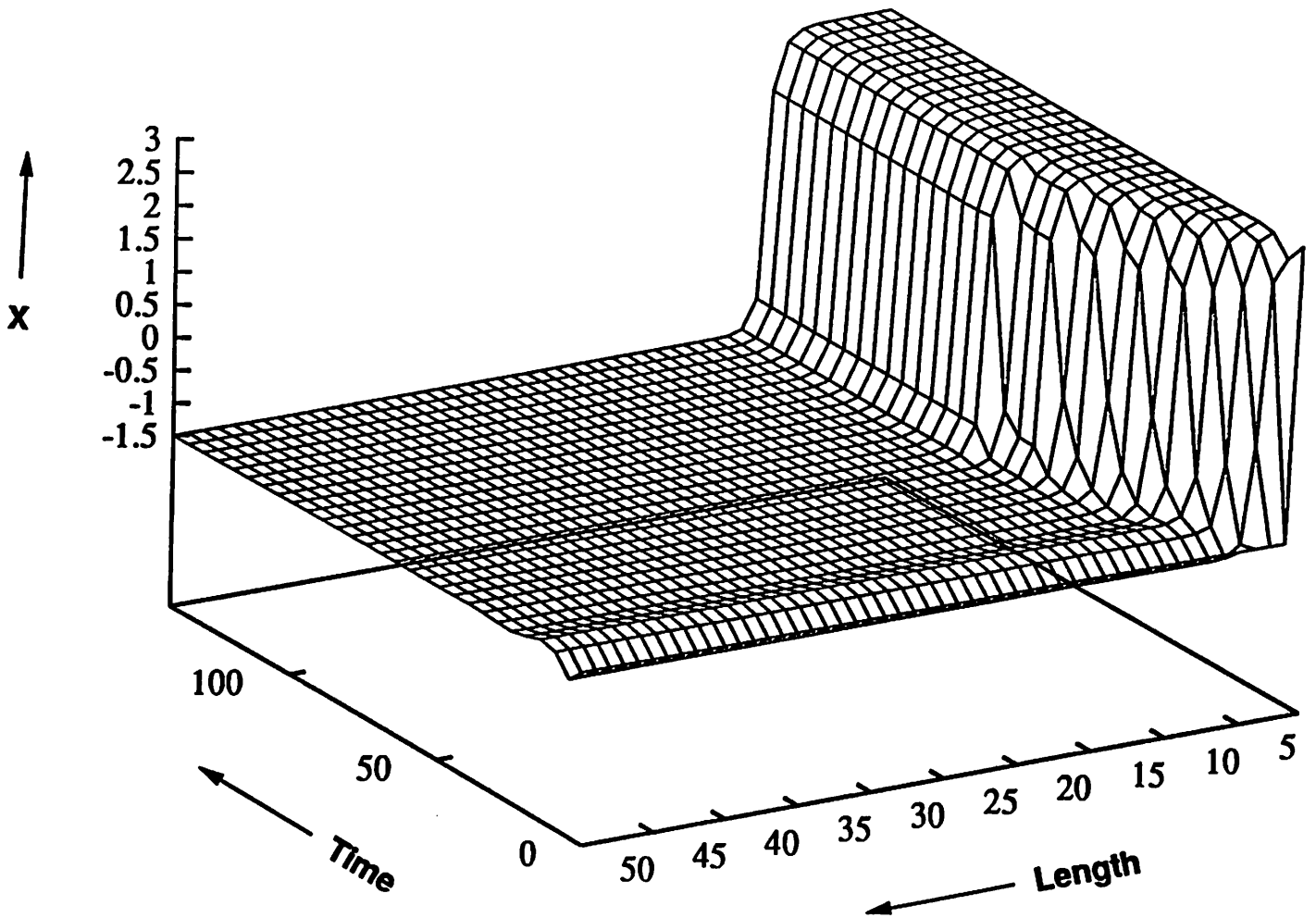
x
3
2.5
2
1.5
1
0.5
0
-0.5
-1
-1.5
100
50
0
Time
50
45
40
35
30
25
20
15
10
5
Length

Figure 7